Published in final edited form as:
Nature. 2012 November 1; 491(7422): 109–113. doi:10.1038/nature11523.

Intrinsically determined cell death of developing cortical interneurons

Derek G. Southwell[1,2,3,9,‡], **Mercedes F. Paredes**[2,4], **Rui P. Galvao**[2,10], **Daniel L. Jones**[1,2], **Robert C. Froemke**[5,11], **Joy Y. Sebe**[2], **Clara Alfaro-Cervello**[6,12], **Yunshuo Tang**[2,3,7], **Jose M. Garcia-Verdugo**[6], **John L. Rubenstein**[8], **Scott C. Baraban**[1,2], and **Arturo Alvarez-Buylla**[1,2,‡]

[1]Neuroscience Graduate Program, University of California, San Francisco, California, 94143, USA

[2]Departments of Neuroscience and Neurosurgery, and the Eli and Edythe Broad Center of Regeneration Medicine and Stem Cell Research; University of California, San Francisco, California, 94143, USA

[3]Medical Scientist Training Program, University of California, San Francisco, California, 94143, USA

[4]Department of Neurology, University of California, San Francisco, California, 94143, USA

[5]Department of Otolaryngology, Coleman Memorial Laboratory and W.M. Keck Foundation Center for Integrative Neuroscience, University of California, San Francisco, California, 94143, USA

[6]Instituto Cavanilles, Universidad de Valencia, Valencia, 46071, Spain

[7]Biomedical Sciences Graduate Program, University of California, San Francisco, California, 94143, USA

[8]Department of Psychiatry and the Eli and Edythe Broad Center of Regeneration Medicine and Stem Cell Research; University of California, San Francisco, California, 94143, USA

Abstract

Cortical inhibitory circuits are formed by GABAergic interneurons, a cell population that originates far from the cerebral cortex in the embryonic ventral forebrain. Given their distant developmental origins, it is intriguing how the number of cortical interneurons is ultimately determined. One possibility, suggested by the neurotrophic hypothesis[1-5], is that cortical interneurons are overproduced, and then following their migration into cortex, excess interneurons are eliminated through a competition for extrinsically derived trophic signals. Here we have characterized the developmental cell death of mouse cortical interneurons in vivo, in vitro, and

[‡]To whom correspondence should be sent: dereksouthwell@gmail.com and abuylla@stemcell.ucsf.edu.
[9]Present address: Department of Neurosurgery, Stanford University School of Medicine, Stanford, California, 94305, USA
[10]Present address: Department of Molecular Biology, University of Oregon, Eugene, Oregon, 97403, USA
[11]Present address: Molecular Neurobiology Program, The Helen and Martin Kimmel Center for Biology and Medicine at the Skirball Institute of Biomolecular Medicine, Departments of Otolaryngology, Physiology and Neuroscience, New York University School of Medicine, New York, New York, 10016, USA
[12]Present address: Cambridge Centre for Brain Repair, Department of Clinical Neurosciences and Stem Cell Institute, University of Cambridge, Cambridge, CB2 0PY, United Kingdom

Author contributions D.S. and A.A. devised experiments. D.S. performed all experiments, with the exception of the following: M.P. performed in vitro culture experiments and measurements of Ki67 labeling, R.G. collected cleaved caspase-3 counts in GAD67-GFP mice, C.A. and J.G. produced electron micrographs, Y.T. performed cell transplantations for the examination of Ki67 labeling, and D.J., J.S. and R.F. performed electrophysiologic recordings. D.S. and A.A. wrote the manuscript.

Declaration of competing interests The authors declare no competing interests.

following transplantation. We found that 40% of developing cortical interneurons were eliminated through *Bax- (Bcl-2 associated X-)* dependent apoptosis during postnatal life. When cultured in vitro or transplanted into the cortex, interneuron precursors died at a cellular age similar to that at which endogenous interneurons died during normal development. Remarkably, over transplant sizes that varied 200-fold, a constant fraction of the transplanted population underwent cell death. The death of transplanted neurons was not affected by the cell-autonomous disruption of TrkB (tropomyosin kinase receptor B), the main neurotrophin receptor expressed by central nervous system (CNS) neurons[6-8]. Transplantation expanded the cortical interneuron population by up to 35%, but the frequency of inhibitory synaptic events did not scale with the number of transplanted interneurons. Together, our findings indicate that interneuron cell death is intrinsically determined, either cell-autonomously, or through a population-autonomous competition for survival signals derived from other interneurons.

We first characterized the developmental cell death of cortical interneurons by measuring the expression of the apoptotic marker, cleaved caspase-3, in GAD67-GFP mice[9] (Figure 1a). The number of cleaved caspase-3-labeled neocortical GAD67-GFP neurons increased from postnatal days 1 to 5 (P1 to P5), reached a maximum around P7, and declined towards zero by approximately P15 (Figure 1b; Analysis of Variance (ANOVA), $F = 84.0$ and $P < 0.0001$). The majority (75%) of cleaved caspase-3-positive cells were observed between P7 and P11 (Figure 1b), approximately 11 to 18 days after the cells were produced in the embryonic ventral forebrain[10]. The temporal profile of cleaved caspase-3 expression in GAD67-GFP cells was similar to that observed across the total cellular population of the neocortex (Figure S2), which may preserve the relative sizes of different cellular populations[11]. Because the GAD67-GFP knock-in reduces brain gamma-aminobutyric acid (GABA) content by approximately 20 to 40%[9], we examined whether this in turn affected cell death in GAD67-GFP mice. Across the entire cellular population of the neocortex, neither the temporal profile nor the extent of apoptosis was significantly different between GAD67-GFP mice and wild type mice (Figure S3).

We next measured the GAD67-GFP population size during postnatal life and adulthood (Figure 1c). The number of GAD67-GFP neurons reached a maximum around P5 (mean, $1.65 \pm 0.03 \times 10^6$ cells), and then declined by approximately 40% during the period of interneuron cell death (Figure 1b), reaching a stable size of $1.01 \pm 0.02 \times 10^6$ cells by P120 (mean; ANOVA, $F = 32.1$ and $P < 0.0001$). The developmental cell death of cortical interneurons depended on Bax function: at P7, when GAD67-GFP cell death reached a maximum in wild type mice (Figure 1b), GAD67-GFP cell death was nearly absent in $Bax^{-/-}$;GAD67-GFP mutants[12] (Figure 1d; Student's t-test, $P = 0.0034$). Between P5 and P120, the cortical GAD67-GFP population did not decline in *Bax* mutants (Figure 1e; ANOVA, $F = 2.28$, $P = 0.18$), and, at P120, the cortical interneuron population was 33% smaller in wild type GAD67-GFP mice than in $Bax^{-/-}$;GAD67-GFP littermates ($1.02 \pm 0.04 \times 10^6$ cells versus $1.52 \pm 0.08 \times 10^6$ cells, respectively; Student's t-test, $P = 0.0041$). In wild type and *Bax* mutant mice, similar proportions of GAD67-GFP neurons were labeled by parvalbumin, somatostatin, neuropeptide Y, and calretinin (Figure S4), indicating that *Bax*-dependent cell death occurred uniformly across neurochemically defined interneuron subtypes. These findings indicate that *Bax*-dependent programmed cell death eliminates roughly 40% of neocortical interneurons during postnatal life.

After characterizing neocortical interneuron cell death in vivo, we examined whether neocortical interneurons undergo a similar pattern of cell death in vitro. We placed interneuron precursors from the embryonic day 13.5 (E13.5) GAD67-GFP medial ganglionic eminence (MGE) onto P0 to P2 neocortical feeder layers[13] (Figure 2a), and quantified the expression of cleaved caspase-3 expression at various timepoints (Figure 2b).

GAD67-GFP neurons underwent cell death in vitro, with cleaved caspase-3 expression reaching a maximum at 13 days (Figure 2c; ANOVA, $F = 9.12$ and $P < 0.0001$). Approximately 66% of cell death occurred between 11 and 15 days in vitro (DIV), around which time the GAD67-GFP cell number declined by approximately 30% (Figure 2d; ANOVA, $F = 4.53$ and $P = 0.0012$). As previously mentioned, in vivo, the majority of interneuron cell death occurred between P7 and 11, when the developing cells were likewise between 11 and 18 days old (Figure 1b). Interneuron cell death thus manifests in vitro, with a temporal pattern resembling that observed in vivo.

We next transplanted embryonic interneuron precursors into the postnatal neocortex during the period of endogenous interneuron cell death[14, 15]. We postulated that, if the timing of interneuron cell death reflects the maturation of interneurons into a trophic signal-dependent state, then transplanted interneuron precursors would undergo developmental cell death asynchronously from endogenous interneurons. We transplanted 5×10^5 cells from the MGE of E13.5 to E14.5 beta-actin:GFP mice[16] into P3 wild type recipients (Figure S5) and then quantified cleaved caspase-3 expression at various timepoints after transplantation. Given that mouse gestation ends around E19, the transplanted interneuron precursors were approximately 6 to 10 days younger than their endogenous counterparts[10]. As previously described[14, 15, 17], transplanted MGE cells dispersed in the recipient cortex, developed the morphological features of GABAergic interneurons (Figure S5), and formed synaptic contacts with recipient neurons (Figure S6). We did not observe Ki-67 labeling of the transplanted interneuron precursors, indicating that the cells did not proliferate in the recipient (Figure S7). Cleaved caspase-3 expression increased 200% in the transplanted population between 7 and 15 DAT, reached a maximum at 15 DAT, then declined to undetectable levels by 45 DAT (Figures 2e and 2f; ANOVA, $F = 17.79$ and $P < 0.0001$). By contrast, in endogenous cells of the recipient neocortex, cleaved caspase-3 expression reached a relative maximum at 7 DAT, then declined approximately 80% between 7 and 15 DAT (Figure S8; ANOVA, $F = 401.20$ and $P < 0.0001$). The addition of transplanted cells did not affect endogenous cell death, as cleaved caspase-3 expression was similar between hemispheres that received transplanted cells and hemispheres that received media vehicle injections (Figure S8; Student's t-test, $P = 0.76$ (7 DAT), $P = 0.83$ (15 DAT), $P = 0.89$ (25 DAT), $P = 0.67$ (45 DAT)). Transplanted interneuron cell death thus reached a maximum around 15 DAT, when the transplanted cells reached a cellular age equivalent to that of endogenous interneurons during the peak of normal developmental cell death (Figures 1b and 2f). Taken together with the in vitro data (Figures 2a-2d), these findings suggest that interneuron cell death is timed by the intrinsic maturational state of the developing cells.

We also used heterochronic transplantation to introduce varying numbers of embryonic interneuron precursors into the neocortex. We expected that, if interneuron cell death is determined by intercellular competition for extrinsically derived signals, then the amount of interneuron cell death should increase with larger transplant sizes. Surprisingly, however, across initial transplant sizes that varied 200-fold (5×10^3, 5×10^4, 5×10^5, and 10^6 cells), similar fractions of the transplanted cells survived in the recipient neocortical hemisphere at 60 DAT (20.8 ± 2.4%, 22.2 ± 1.4%, 17.8 ± 0.6% and 15.3 ± 0.3%, respectively; Figure 3a; ANOVA, $F = 0.34$ and $P = 0.12$). When 10^6 or 2×10^6 cells were transplanted, similar numbers of cells survived ($1.65 \pm 0.18 \times 10^5$ cells versus $1.53 \pm 0.01 \times 10^5$ cells, respectively; Student's t-test, $P = 0.58$), suggesting that the neocortical hemisphere has a limited capacity for approximately 1.6×10^5 additional interneurons. However, when the initial transplant size was far smaller than this theoretical limit, transplanted cell death still occurred, and it occurred at a constant rate. This finding indicates that interneuron cell death is not governed by competition for limited trophic signals derived from other cell types.

To further examine whether soluble neurotrophic signals regulate interneuron cell death, we studied the survival of mutant interneurons lacking the neurotrophin receptor, TrkB. We transplanted interneuron precursors from *TrkB*$^{-/-}$ donors[18] into P2 wild type recipients and examined the survival of the cells at 60 DAT. Surprisingly, the survival of transplanted *TrkB*$^{-/-}$ interneurons was similar to that of transplanted wild type cells (Figure 3b; 2.32 ± 0.32 × 10^4 wild type cells versus 2.20 ± 0.20 × 10^4 *TrkB*$^{-/-}$ cells; Student's t-test, P = 0.75), indicating that the cell death of transplanted interneurons is not governed by neurotrophin signaling through TrkB. This finding is consistent with other reports suggesting that the death of developing CNS neurons is regulated by mechanisms other than neurotrophin signaling[6, 19].

To confirm that transplanted interneuron cell death occurred through Bax-dependent apoptosis, we examined the survival of transplanted *Bax*$^{-/-}$ mutant cells[12], and compared their survival to that of transplanted wild type and *Bax*$^{+/-}$ and cells. We pooled counts of wild type and *Bax*$^{+/-}$ interneurons because endogenous interneuron cell death was not disrupted in P20 *Bax*$^{+/-}$ GAD67-GFP mutants (8.88 ± 0.03 × 10^5 wild type cells versus 9.63 ± 0.04 × 10^5 *Bax*$^{+/-}$ cells; Student's t-test, P = 0.20). At 60 DAT into P2 recipients, transplanted *Bax* null interneurons survived in greater numbers than transplanted *Bax* heterozygous and wild-type interneurons (Figure 3c; 4.31 ± 0.21 × 10^4 *Bax*$^{+/-}$ and wild type cells versus 9.11 ± 1.63 × 10^4 wild type cells; Student's t-test, P = 0.03), indicating that the death of transplanted interneurons, like that of endogenous interneurons, occurs at least partially through a Bax-dependent mechanism.

While our transplantation experiments strongly suggested that interneuron cell death is not determined through competition for extrinsic survival signals, it was possible that the transplanted cells competed with endogenous cells, and the survival of the transplanted interneurons occurred at the expense of endogenous interneuron survival. To examine this possibility, we transplanted 10^6 beta-actin:DsRed MGE cells[20] to one neocortical hemisphere of P2 to P3 GAD67-GFP recipients, and then compared the number of endogenous interneurons between the recipient and contralateral control hemispheres (Figure 3d). As expected (Figure 3a), we observed an average of approximately 1.7 × 10^5 transplanted interneurons in the recipient cortical hemisphere at 60 DAT (Figure 3e; mean 1.69 ± 0.41 × 10^5 cells). In the recipient and control hemispheres, we observed equal numbers of endogenous interneurons (Figure 3e; mean endogenous cell count, recipient hemisphere = 4.81 ± 0.12 × 10^5; mean endogenous cell count, control hemisphere = 5.04 ± 0.15 × 10^5; Student's t-test, P = 0.28), consistent with the findings presented in Figure S8, which indicated that transplantation did not affect cleaved caspase-3 expression in endogenous cells. The neocortex is thus able to support approximately 35% additional interneurons, with no effect on the endogenous interneuron population size. This suggests that developmental cell death does not tune the number of developing interneurons towards a cellular limit, as would occur if interneuron number is determined by the availability of limited, extrinsically derived survival signals.

Given that transplantation increases the number of interneurons in the neocortex, it offers a strategy for studying the relationship between interneuron number and cortical inhibition. To explore this relationship, we transplanted varying numbers of interneuron precursors into P2 to P3 recipients, and then performed in vitro patch-clamp recordings on endogenous neocortical pyramidal neurons at 30 to 40 DAT. We recorded the amplitudes and frequencies of spontaneous inhibitory post-synaptic currents (sIPSCs; Figure 4a) and then performed post-hoc quantification of transplanted interneuron cell densities. Consistent with previous findings[15, 17], transplanted interneurons increased the frequency of sIPSCs onto endogenous pyramidal neurons (Figure 4b; controls, 18.4 ± 3.4 Hz; transplant recipients, 31.7 ± 3.9 Hz; Wilcoxon rank-sum test, P = 0.02). The amplitudes of inhibitory events,

however, were not significantly increased by transplantation (Figure 4b; controls, 37.3 ± 1.9 pA; transplant recipients, 42.4 ± 2.5 pA; Wilcoxon rank-sum test, P = 0.22). Remarkably, inhibitory event frequencies did not increase with transplanted interneuron density (linear regression analysis, slope = 0.0003 and r^2 = 0.0003; Figure 4c). Thus, the extent of cortical inhibition is more likely determined by mechanisms that adjust synaptic strength and number, rather than mechanisms that govern interneuron population size. These findings indicate that transplantation can add a limited amount of new inhibition to the neocortex, and this limit is reached with transplanted cell numbers much smaller than that which the neocortex can support.

In summary, our findings suggest that interneuron cell death is regulated by intrinsically defined mechanisms. When interneuron precursors were cultured in vitro or heterochronically transplanted, they died when they reached a cellular age equivalent to that of endogenous interneurons during the peak of endogenous interneuron cell death (Figures 1 and 2). This suggests that interneuron cell death is timed by the expression of a maturational program intrinsic to interneurons, rather than the developmental state of the cortex itself. Likewise, the extent of interneuron cell death appears to be intrinsically defined: across a range of transplant sizes, a constant fraction of the transplanted interneurons died in the recipient cortex, even when the transplant size was significantly below the number of interneurons the cortex could support (Figure 3). As such, interneuron cell death is unlikely to follow from intercellular competition for limiting survival signals derived from other cell types.

We propose two mechanisms that may govern the developmental cell death of cortical interneurons (Figure S1). In the first, which we refer to as ‘cell-autonomous,’ interneuron cell death is intrinsically determined within each embryonic interneuron precursor. In this scenario, interneuron precursors would be individually destined to die in a manner independent from their interactions with other cell types. For example, the production of interneurons could occur with a certain rate of error[21] such that a fraction of defective interneuron precursors cannot survive past a certain cellular age. Similarly, a fixed fraction of interneuron precursors may be cell-autonomously programmed to die during a specific stage of their development. Alternatively, in a ‘population-autonomous’ mechanism, developing interneurons may require and compete for limiting survival signals produced by other isochronic interneurons. These neurotrophic signals, which may be obtained via cell-cell contact, synaptic transmission, or neurotrophin signaling independent of TrkB, would be present in a quantity that scales to the number of isochronic developing interneurons. Either a cell-autonomous or population-autonomous mechanism could account for why (1) cell death occurred at a constant rate across broad range of interneuron transplant sizes, and, (2) the survival of endogenous interneurons was not affected by the transplantation of additional interneurons.

Interneurons play a critical role in cortical physiology, and their dysfunction has been implicated in neurological disorders such as epilepsy, schizophrenia, and Alzheimer’s disease[22-24]. The detailed examination of interneuron cell death is thus expected to yield new insights into cortical development, the pathophysiology of brain disorders, and the therapeutic application of neuronal transplantation.

Full methods

Animals

All protocols and procedures followed the guidelines of the Laboratory Animal Resource Center at the University of California, San Francisco. Neonatal GAD67-GFP mice were produced by crossing heterozygous GAD67-GFP(Δneo) mice[9] to wild type C57Bl/6 mice.

Bax$^{-/-}$;GAD67-GFP mice were produced by crossing *Bax*$^{+/-}$ mice[12] to *Bax*$^{+/-}$;GAD67-GFP mice. Embryonic donor tissue was produced by crossing CD-1 wild type mice to homozygous, beta-actin:green fluorescent protein-expressing (GFP) mice[16] and homozygous beta-actin:Discosoma red fluorescent protein-expressing (DsRed) mice[20]. Adult C57Bl/6 and CD-1 breeder mice were obtained from Charles River Laboratories. *TrkB*$^{-/-}$;GFP donor tissue was obtained from embryos produced by crossing *TrkB*$^{+/-}$ mice[18] to *TrkB*$^{+/-}$;GFP mice. *Bax*$^{-/-}$;GFP donor tissue was obtained from embryos produced by crossing *Bax*$^{+/-}$ mice[12] to *Bax*$^{-/-}$;GFP mice. Adult C57Bl/6 and CD-1 breeder mice were obtained from Charles River Laboratories. *Bax*$^{+/-}$ mice were obtained from Jackson Laboratories. GAD67-GFP offspring were genotyped under an epifluorescence dissection microscope (Leica), while *Bax* mice and *TrkB* mice were genotyped using polymerase chain reaction. Unless noted, all cell transplantation experiments were performed using wild type C57Bl/6 recipient mice. All mice were housed under identical conditions.

Preparation of primary MGE cultures and feeder cell layers

Primary cortical cultures were prepared as previously described[13]. The neocortex was dissected from P0 to P2 CD1 mice, macerated using fine forceps, then trypsinized in the presence of Leibovitz L-15 medium (UCSF Cell Culture Facility) and DNase (1 U/ml; Promega, Madison, WI). The tissue was triturated using a pipette, and then resuspended in DMEM-F12 media (UCSF Cell Culture Facility) containing 10% fetal bovine serum (Hyclone). Fifty thousand cells were added to each well of 8-well chamber slides (70 mm^2; BD Falcon) coated with polylysine (10 g/ml) and laminin (5 g/ml; UCSF Cell Culture Facility). Cultures were maintained at 37°C in the presence of 5% carbon dioxide and ambient oxygen.

Medial ganglionic eminences were dissected from E13.5 GAD67-GFP embryos and mechanically dissociated in a solution of Leibovitz L-15 medium and DNase. The resultant cell suspension was then concentrated by brief centrifugation and placed in N5 medium (DMEM-F12 with glutamax, 100× N2 supplement (Invitrogen)), containing DNAse, bovine pituitary extract (35 ug/ml; Invitrogen), human epidermal growth factor (20 ng/ml), human fibroblast growth factor-2 (20 ng/ml; Preprotech), and fetal 5% bovine serum (Hyclone). The MGE cells were added to wells containing feeder layers grown for 24 hours (5×10^3 cells per well). The cultures were thereafter maintained in Neurobasal/B27 medium (Invitrogen). We measured proliferation of the cultured neurons by immunostaining for the proliferative marker, phospho-histone H3 (pH3). At 4 DIV, 1.5 ± 0.9% of GAD67-GFP cells expressed pH3. Proliferation was nearly absent at later timepoints, as 0.2 ± 0.2% of cells were pH3-positive at 14 DIV, and no pH3-positive cells were observed at 21 DIV.

Cell transplantation

The ventricular and subventricular layers of the medial ganglionic eminence (MGE) were dissected from embryonic day 13.5 to 14.5 (E13.5 to E14.5) donor embryos. The timepoint when the sperm plug was detected was considered E0.5. Embryonic MGE explants were dissected in Leibovitz L-15 medium containing DNaseI (100 μg/ml). Unless otherwise noted, the explants were mechanically dissociated into a single cell suspension by repeated pipetting. The dissociated cells were then concentrated by centrifugation (3 minutes, 1000 × g). For the transplantation of *TrkB* and *Bax* mutant interneuron precursors, whole MGE explants were directly transplanted. Concentrated cell suspensions (~10^3 cells/nl) or whole MGE explants were loaded into beveled glass micropipettes (~50 μm tip diameter; Wiretrol 5 μl, Drummond Scientific Company). Micropipettes were positioned at an angle of 35-45 degrees from vertical in a stereotactic injection apparatus. Recipient mice were anesthetized by hypothermia and positioned in a clay head mold that stabilized the skull. The concentrated cell suspensions were injected into the neocortex at a depth of 700 μm, as

depicted in Figure S5. In the experiments described in Figures 3d and 3e, the contralateral hemispheres received a control, injection of L-15 containing DNase. After the injections were completed, transplant recipients were placed on a warm surface to recover from hypothermia. The mice were then returned to their mothers until they were perfused or weaned (P20).

Immunostaining

Cell cultures were fixed in 4% paraformaldehyde for 10 minutes, and immunostaining was performed directly in 8-well chamber slides. Mice were transcardially perfused with 4% paraformaldehyde, then the brains were removed, postfixed overnight in 4% paraformaldehyde, and cryoprotected in 25% sucrose. Coronal brain sections were cut using a frozen sliding microtome. For immunostaining of cell cultures, tissue blocking and antibody incubations were done using a solution of 2% bovine serum albumin, 1% normal goat serum, and 0.1% Triton X-100 in phosphate-buffered saline (PBS). For immunostaining of floating sections, tissue blocking and antibody incubations were done using a solution of 2% bovine serum albumin, 8% normal goat serum, and 0.5% Triton X-100 in PBS. Samples were blocked for 1 hour at room temperature, incubated in primary antibody solutions overnight at 4°C, and incubated in secondary antibody solutions for 2 hours at room temperature. Immunostaining was performed with the following primary antibodies: chicken anti-GFP (1:500; Aves Labs), rabbit anti-cleaved caspase-3 (1:500; Cell Signaling Technologies), mouse anti-Tuj1 (1:500; Covance), mouse anti-GFAP (1:1000; Millipore), rabbit anti-Olig-2 (1:1500; Millipore), rabbit anti-phosphohistone-H3 (1:750; Millipore), and rabbit anti-DsRed (1:500; Clontech). The following secondary antibodies were used for fluorescence labeling: Alexa Fluor 488 goat anti-chicken, Alexa Fluor 594 donkey anti-rabbit (Molecular Probes). For diaminobenzidine labeling, a peroxidase-conjugated goat anti-chicken secondary antibody was used (Sigma). Diaminobenzidine-(DAB-) labeled sections were developed in 0.3% diaminobenzidine and 0.01% hydrogen peroxide for approximately 30 minutes. After the primary and secondary antibody incubations were finished, sections were washed four times in PBS. Floating sections were mounted on glass slides and coverslipped.

Cell quantification

For cell counts in vitro, phospho-histone-3-positive cells, cleaved caspase-3-positive cells and GAD67-GFP cells were directly counted using an Olympus AX70 microscope with a 20× objective. At each timepoint, cell counts were made in 4 separate wells. In each well, counts were obtained from five different fields. For cell counts in vivo, cleaved caspase-3 expressing cells, GAD67-GFP cells, and transplanted cells were counted in all layers of the entire neocortex. Cell counts were not performed in other areas of the cortex such as the olfactory bulb, piriform cortex or hippocampus. At all timepoints, only transplanted cells that expressed neuronal morphologies were counted. As previously described, the vast majority of cells transplanted from the E13.5 to E14.5 MGE exhibited neuronal morphologies in the recipient[14, 15, 17]. Cleaved caspase-3-positive cells and transplanted interneuron precursors (initial transplant sizes of less than or equal to 10^5 cells) were directly counted in every sixth coronal section (except for the cleaved caspase-3 counts in transplant recipients, which were made in every second coronal section) using an Olympus AX70 microscope with a 20× objective. The raw cell counts were then multiplied by the inverse of the section sampling frequency (6 or 2, respectively) to obtain an estimate of total cell number. To quantify populations of larger sizes (endogenous GAD67-GFP cells and initial transplant sizes greater than or equal to 5×10^5 cells), design-based stereology was performed on DAB-labeled sections (endogenous GAD67-GFP cells) or fluorescently labeled (transplanted cells) using an optical fractionator (StereoInvestigator, MicroBrightField, Inc.) and a Nikon Eclipse microscope with a 100x objective.

Histological imaging

Images were obtained using a confocal microscope (Leica SP5). Figures 1a, 2a, 2b, 2f, 2g and 3d depict flattened Z-series of confocal slices (1a, 6 slices, 0.8 μm per slice; 2a and 2b, 5 slices, 8 μm per slice; 2f, 10 slices, 1 μm per slice; 2g, 7 slices, 1.1 μm per slice; 3d 9 slices, 1.2 μm per slice). Images were adjusted for brightness and contrast with Adobe Photoshop CS3 (Adobe Systems Inc.).

Electron microscopy

Mice were transcardially perfused with 4% paraformaldehyde and 0.5% glutaraldehyde. The brains were removed, postfixed overnight in 4% paraformaldehyde, and cryoprotected in 25% sucrose. Fifty μm coronal brain sections were cut using a frozen sliding microtome and then freeze-thawed three times in methyl-butane and dry ice. Sections were washed in phosphate buffer (PB), blocked 1h at room temperature in 0.3% bovine serum albumin-A (BSA; Aurion) in PB and incubated for 72h at 4°C in 1:200 chicken anti-GFP in PB. Sections were washed in PB and blocked in 0.5% BSA and 0.1% fish gelatin for 1h at room temperature, and then incubated for 24h at 4°C in blocking solution plus 1:50 colloidal gold-conjugated anti-chicken secondary antibody (Aurion). Sections were washed in PB containing 2% sodium acetate at room temperature. Silver enhancement was performed according to the manufacturer's instruction (Aurion), and sections were washed in 2% sodium acetate. To stabilize the silver particles, the sections were immersed in 0.05% gold chloride for 10 minutes at 4°C and washed in sodium thiosulfate. Sections were then post-fixed in 2% glutaraldehyde for 30 minutes at room temperature. Sections were contrast enhanced in 1% osmium and 7% glucose then embedded in araldite. Semi-thin 1.5μm sections were prepared and selected using a light microscope before being re-embedded for ultrathin sectioning (70 nm). Electron micrographs were obtained under a Fei microscope (Tecnai-Spirit) using a digital camera (Morada, Soft-imaging System).

Electrophysiology

Fluorescently labeled (GFP or DsRed) E13.5 MGE cells were transplanted into P2 to P3 wild type C57Bl/6 recipients. The initial transplant size was varied from approximately 10^3 to 5×10^5 cells, in order to produce a recipient group that ranged with respect to the transplanted population size. Coronal brain slices (300 μm thickness) were prepared from recipient mice 30 to 40 DAT of either vehicle (L-15 medium) or MGE cells. Slices were perfused with carbogen-bubbled artificial cerebrospinal fluid containing (in mM): 124 NaCl, 3 KCl, 1.25 NaH_2PO4-H_2O, 2 $MgSO_4$-$7H_2O$, 26 $NaHCO_3$, 10 dextrose, and 2 $CaCl_2$, and maintained at 33-34 C. Spontaneous inhibitory postsynaptic currents were recorded from layer 2/3 pyramidal cells in the somatosensory cortex using Clampex software (Molecular Devices) at a gain of 5 and a filter at 1 kHz. Patch electrodes (3-5 MΩ) were filled with (in mM): 140 CsCl, 1 $MgCl_2$, 10 HEPES, 11 EGTA, 2 NaATP, 0.5 Na_2GTP and 1.25 QX-314. Pyramidal neurons were held at −60 mV and bathed in 25 μM APV and 20 μM DNQX (Sigma) to block glutamate receptors. Gabazine (100 μM) was applied to the bath at the end of the experiment to confirm the inhibitory nature of recorded events. The series resistance was measured after each recording, and data were discarded if the resistance changed by more than 20%, or if the series resistance was found to be greater than 20 MΩ. MiniAnalysis software (Synaptosoft) was used to quantify sIPSC frequency and amplitude. All electrophysiology was done with the experimenter blinded to the number of transplanted interneurons. After the recordings were completed, the slices were placed in 4% paraformaldehyde overnight, post-fixed in 25% sucrose, and then cut into 50 μm sections on a vibratome. The number of transplanted interneurons in the neocortex of a 50 μm slice was counted for each recipient. To obtain the cell density, the cell count was then divided by the area of neocortex in the coronal section.

Statistical analysis

The Student's t-test was used to compare cell counts between two groups. An analysis of variance was used to test for differences among three or more groups. With the exception of the electrophysiology experiments, all statistical analyses were performed using Prism 4.0 (Graphpad). The statistical analysis of the electrophysiology data was performed using Sigma Plot 12 (Systat Software Inc.). A Wilcoxon rank-sum test and linear regression analysis were used to analyze the sIPSC data.

Supplementary Material

Refer to Web version on PubMed Central for supplementary material.

Acknowledgments

We thank Yuchio Yanagawa for GAD67-GFP mice, Lou Reichardt for *TrkB* mutant mice, and Ricardo Romero for technical contributions. D.S. and M.P. were supported by training grants from the California Institute for Regenerative Medicine. This work was supported by the John G. Bowes Research Fund (A.A.), the Spanish Ministry of Science and Innovation (J.G., SAF-2008-01274), and the National Institutes of Health (J.S., F32NS061497; J.R., S.B. and A.A., R01 NS071785; A.A-B., R01 NS048528).

References

1. Buss RR, Sun W, Oppenheim RW. Adaptive roles of programmed cell death during nervous system development. Annu. Rev. Neurosci. 2006; 29:1–36. [PubMed: 16776578]
2. Oppenheim RW. Cell death during development of the nervous system. Annu. Rev. Neurosci. 1991; 14:453–501. [PubMed: 2031577]
3. Hamburger V, Levi-Montalcini R. Proliferation, differentiation and degeneration in the spinal ganglia of the chick embryo under normal and experimental conditions. J. Exp. Zool. 1949; 111:457–501. [PubMed: 18142378]
4. Levi-Montalcini R. The development of the acoustico-vestibular centers in the chick embryo in the absence of the afferent root fibers and of descending fiber tracts. J. Comp. Neurol. 1949; 91:209–241. [PubMed: 15408222]
5. Boya P, De la Rosa EJ. Cell death in early neural life. Birth Def. Res. 2005; 75:281–293.
6. Nikoletopoulou V, et al. Neurotrophin receptors TrkA and TrkC cause neuronal death whereas TrkB does not. Nature. 2010; 467:59–64. [PubMed: 20811452]
7. Polleux F, Whitford KL, Dijkhuizen PA, Vitalis T, Ghosh A. Control of cortical interneuron migration by neurotrophins and PI3-kinase signaling. Development. 2002; 129:3147–3160. [PubMed: 12070090]
8. Gorba T, Wahle P. Expression of TrkB and TrkC but not BDNF mRNA in neurochemically identified interneurons in rat visual cortex in vivo and in organotypic cultures. Eur. J. Neurosci. 1999; 11:1179–1190. [PubMed: 10103114]
9. Tamamaki N, et al. Green fluorescent protein expression and colocalization with calretinin, parvalbumin, and somatostatin in the GAD67-GFP knock-in mouse. J. Comp. Neurol. 2003; 467:60–79. [PubMed: 14574680]
10. Wonders CP, Anderson SA. The origin and specification of cortical interneurons. Nat. Rev. Neurosci. 2006; 7:687–696. [PubMed: 16883309]
11. Sahara S, Yanagawa Y, O'Leary DDM, Stevens CF. The fraction of cortical GABAergic neurons is constant from near the start of cortical neurogensis to adulthood. J Neurosci. 2012; 32:4755–4761. [PubMed: 22492031]
12. Knudson CM, Tung KS, Tourtellote WG, Brown GA, Korsmeyer SJ. Bax-deficient mice with lymphoid hyperplasia and male germ cell death. Science. 1995; 270:96–99. [PubMed: 7569956]
13. Xu Q, Cobos I, De la Cruz E, Rubenstein JL, Anderson SA. Origins of cortical interneuron subtypes. J. Neurosci. 2004; 24:2612–2622. [PubMed: 15028753]

14. Wichterle H, Garcia-Verdugo JM, Herrera DG, Alvarez-Buylla A. Young neurons from medial ganglionic eminence disperse in adult and embryonic brain. Nat. Neurosci. 1999; 2:461–466. [PubMed: 10321251]
15. Alvarez-Dolado M, et al. Cortical inhibition modified by embryonic neural precursors grafted into the postnatal brain. J. Neurosci. 2005; 26:7380–7389. [PubMed: 16837585]
16. Hadjantonakis A, Gertenstein M, Ikawa M, Okabe M, Nagy A. Generating green fluorescent mice by germline transmission of green fluorescent ES cells. Mech. Devel. 1998; 76:79–90. [PubMed: 9867352]
17. Southwell DG, Froemke RC, Alvarez-Buylla A, Stryker MP, Gandhi SP. Cortical plasticity induced by inhibitory neuron transplantation. Science. 2010; 327:1145–1148. [PubMed: 20185728]
18. Galvao RP, Garcia-Verdugo JM, Alvarez-Buylla A. Brain-derived neurotrophic factor signaling does not stimulate subventricular zone neurogenesis in adult mice and rats. J. Neurosci. 2008; 28:13368–13383. [PubMed: 19074010]
19. Silos-Santiago, et al. Severe sensory deficits but normal CNS development of newborn mice lacking TrkB and TrkC tyrosine protein kinase receptors. Eur. J. Neurosci. 1997; 9:2045–2056. [PubMed: 9421165]
20. Vintersten K, et al. Mouse in red: Red fluorescent protein expression in mouse ES cells, embryos, and adult animals. Genesis. 2004; 40:241–246. [PubMed: 15593332]
21. Saunders J. Death in embryonic systems. Science. 1966; 154:604–612. [PubMed: 5332319]
22. Cossart R, Bernard C, Ben-Ari Y. Multiple facets of GABAergic neurons and synapses: multiple fates of GABA signaling in epilepsies. Trends Neurosci. 2005; 28:108–115. [PubMed: 15667934]
23. Marin O. Interneuron dysfunction in psychiatric disorders. Nat. Rev. Neurosci. 2012; 13:107–120. [PubMed: 22251963]
24. Verret L, et al. Inhibitory interneuron deficit links altered network activity and cognitive dysfunction in Alzheimer Model. Cell. 2012; 149:708–721. [PubMed: 22541439]

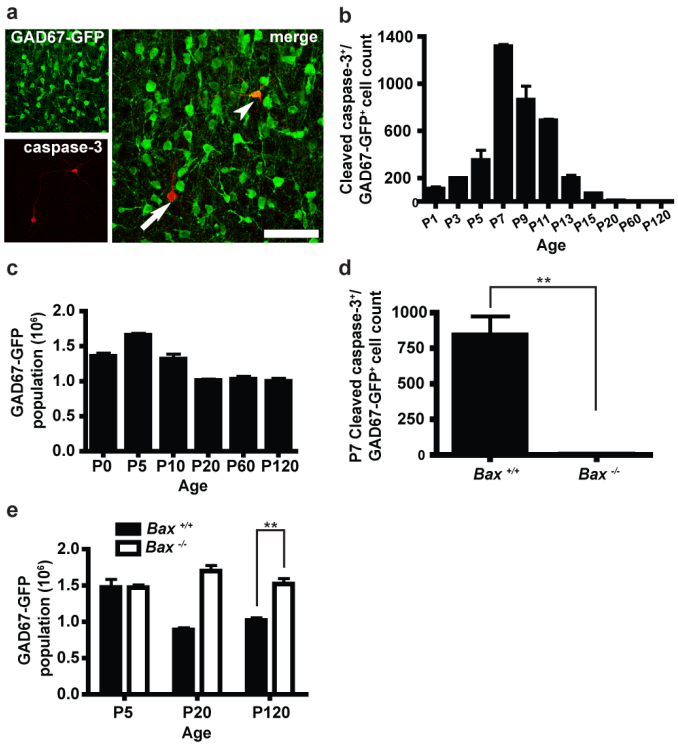

Figure 1. *Bax*-dependent programmed cell death eliminates 40% of developing interneurons from the postnatal mouse neocortex

(a) Cleaved caspase-3 expression (red) observed in GAD67-GFP neurons (green; arrowheads) and other cell types (arrow) of the P7 neocortex. Scale bar, 100 μm (left) and 50 μm (right). **(b)** Temporal profile of cleaved caspase-3 expression in the neocortex of GAD67-GFP mice. Cleaved caspase-3 expression is highest at P7, and declines to nearly undetectable levels by P15 (ANOVA, $F = 84.00$ and $P < 0.0001$; $n = 3$ per timepoint). **(c)** Temporal profile of the neocortical GAD67-GFP population size. Between P5 and P20, the neocortical GAD67-GFP population decreases by approximately 40% (ANOVA, $F = 32.10$ and $P < 0.0001$; $n = 5$ per timepoint). **(d)** The *Bax* mutation disrupts the developmental cell death of cortical interneurons. $Bax^{-/-}$ mice exhibit a 99.8% reduction in the number of cells double labeled by cleaved caspase-3 and GAD67-GFP, as compared to $Bax^{+/+}$;GAD67-GFP littermates (Student's t-test, ** $P < 0.01$; $n = 3$ per genotype). **(e)** The neocortical GAD67-GFP population does not decrease in $Bax^{-/-}$ mice (ANOVA, $F = 2.28$ and $P = 0.18$). At P120, the neocortical GAD67-GFP population is approximately 33% smaller in wild type mice (Student's t-test, ** $P < 0.01$; $n = 3$ per genotype at each timepoint). In all figures, error bars represent the standard error of the mean.

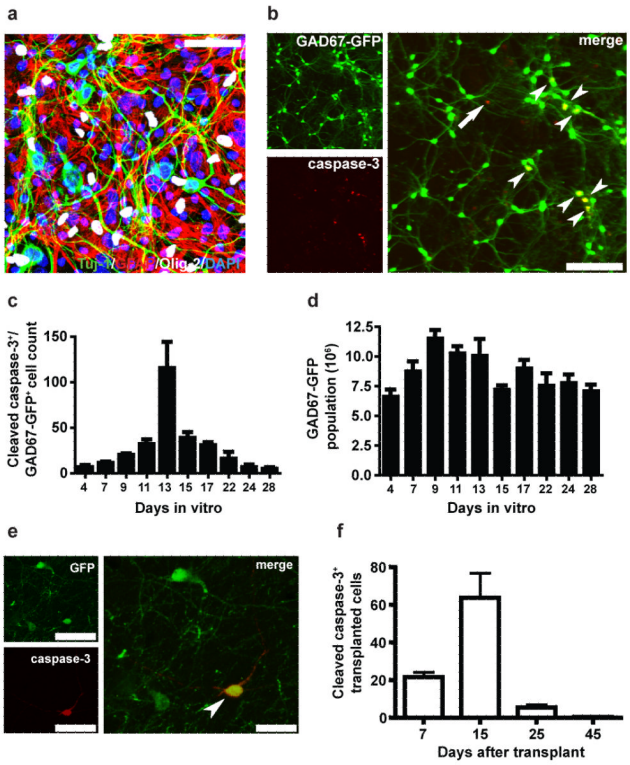

Figure 2. In vitro, and following heterochronic transplantation, interneuron precursors undergo programmed cell death during a period defined by their intrinsic cellular age

(a) Primary feeder layers prepared from P0-P2 neocortex. At 14 days in vitro (DIV), the feeder layer contains neurons (Tuj-1, green), astrocytes (GFAP, red), and oligodendrocytes (Olig-2, white). All cells are labeled by DAPI (blue). Scale bar, 50 μm. **(b)** At 14 DIV, double-labeled cells expressing cleaved caspase-3 (red) and GAD67-GFP (green; arrowheads) are observed along with cells singly labeled by cleaved caspase-3 (arrows). Scale bars, 200 μm. **(c)** Temporal profile of cleaved caspase-3 expression in GAD67-GFP neuronal cultures. Cleaved caspase-3 expression is highest at 13 DIV (ANOVA, $F = 9.12$ and $P < 0.0001$). **(d)** Temporal profile of the GAD67-GFP population size in vitro. The GAD67-GFP population increases in number between 4 and 9 DIV, likely due to cell proliferation (see Methods), reaches a maximum size around 9 to 11 DIV, and then declines approximately 30% before reaching a stable size around 17 to 22 DIV (ANOVA, $F = 4.53$ and $P < 0.01$). **(e)** A transplanted interneuron precursor expressing cleaved caspase-3 (red) and beta-actin:GFP (green; arrowhead) at 15 DAT. Scale bars, 50 μm (left) and 25 μm (right). **(f)** Temporal profile of cleaved caspase-3 expression in transplanted interneuron precursors. Cleaved caspase-3 is highest at 15 DAT, when the transplanted population reaches an intrinsic cellular age similar to that of endogenous interneurons during the peak of normal developmental cell death (Figure 1b; ANOVA, $F = 17.79$ and $P < 0.0001$; $n = 5$ per timepoint). In all figures, error bars represent the standard error of the mean.

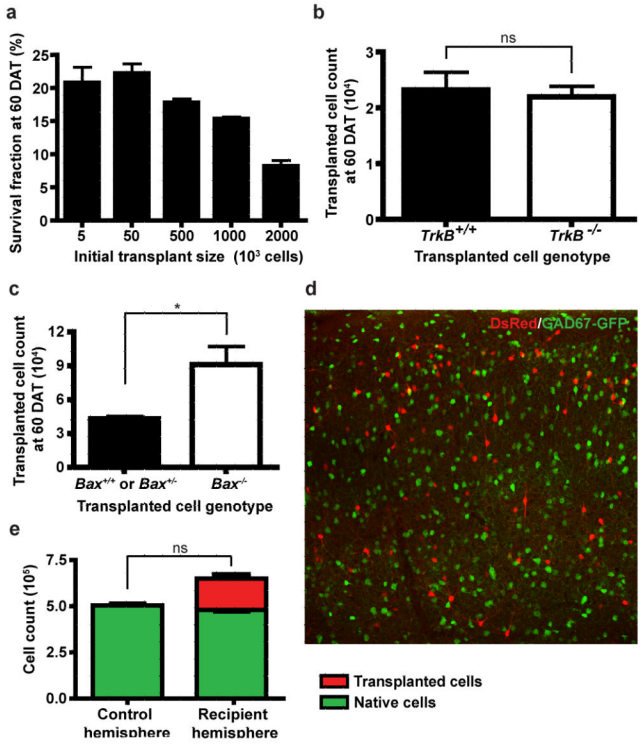

Figure 3. Transplanted interneuron cell death is not governed by competition for survival signals derived from other cell types in the recipient neocortex

(a) Over a broad range of transplant sizes (from 5×10^3 to 1000×10^3 cells) nearly constant fractions of the transplanted populations survive at 60 DAT (approximately 15 to 22%; ANOVA, F = 0.34 and P = 0.12; n = 6, 7, 3, 3 per transplant size, respectively). When the initial transplant size is increased to 2×10^6 cells, a smaller fraction of transplanted cells survives in the recipient neocortex (approximately 8%; n = 3). **(b)** Equal numbers of transplanted *TrkB*$^{-/-}$;beta-actin:GFP interneurons and *TrkB*$^{+/+}$;beta-actin:GFP interneurons survive in the recipient neocortex at 60 DAT (Student's t-test, P = 0.75; n = 5 per genotype). **(c)** Transplanted cortical interneuron cell death occurs through a *Bax*-dependent mechanism. Greater numbers of *Bax*$^{-/-}$;beta-actin:GFP cortical interneurons survive in the recipient cortex at 60 DAT, compared to transplanted *Bax*$^{+/+}$;beta-actin:GFP and *Bax*$^{+/-}$;beta-actin:GFP cortical interneurons (Student's t-test, * P < 0.05; n = 5 wild-type and *Bax*$^{+/-}$; n = 6 *Bax*$^{-/-}$). **(d)** Transplanted beta-actin:DsRed interneurons (red) and endogenous GAD67-GFP neurons (green) at 60 DAT (initial transplant size = 10^6 cells; Scale bar = 150 μm). **(e)** At 60 DAT, transplanted DsRed-labeled interneurons increase the cortical interneuron population size by 34% (Red) without affecting the endogenous GAD67-GFP population (green; Student's t-test, P = 0.28; n = 3). In all figures, error bars represent the standard error of the mean.

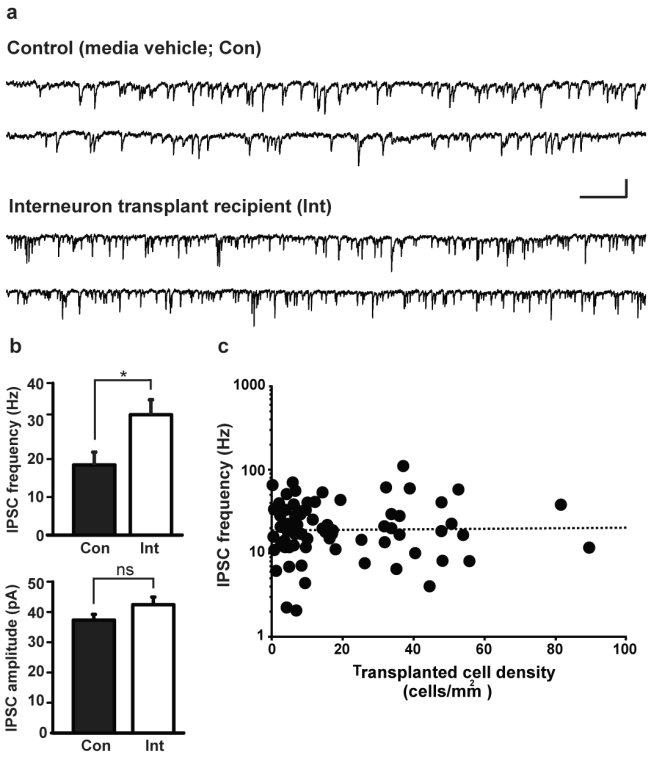

Figure 4. Interneuron population size is not a primary determinant of the level of functional cortical inhibition

(a) Representative traces of spontaneous inhibitory postsynaptic currents (sIPSCs) recorded from endogenous neocortical pyramidal neurons in vitro (media vehicle (Con), top; interneuron transplant recipient (Int), bottom). Vertical scale bar, 40 pA; horizontal scale bar, 200 ms. **(b)** Transplanted interneurons increase the frequency (top), but not the amplitude (bottom) of sIPSCs recorded at 30 to 40 DAT (Wilcoxon rank-sum test, * $P < 0.05$ and $P = 0.22$, respectively; n = 23 recorded cells from control animals, n = 37 recorded cells from interneuron transplant recipients). Mean transplanted cell density for transplant recipient group = 23.3 ± 3.8 cells/mm^2. Error bars represent the standard error of the mean. **(c)** The frequency of sIPSCs onto host pyramidal neurons does not increase with the density of transplanted interneurons (linear regression analysis, slope = 0.0003, $r^2 = 0.0003$).